Cue-based feedback enables remapping in a multiple oscillator model of place cell activity

Joe Monaco[1], **Kechen Zhang**[2], **Hugh T. Blair**[3,4] **James J. Knierim**[1]

[1]Zanvyl Krieger Mind/Brain Institute, [2]Biomedical Engineering Dept., Johns Hopkins University; [3]Psychology Dept. and [4]Brain Research Institute, UCLA

Abstract

Place fields in rat hippocampus consist of both a firing-rate component [6] and a temporal component defined by spike-phase precession relative to local theta [7]. Models based on oscillatory phase interference [e.g., 4 and 5] can account for phase precession, but not for the remapping that can occur when an animal is exposed to novel spatial information. Cue manipulations can induce partial remapping and gradual spatial recoding in which some degree of coherence with previous representations is retained.

Double-rotation experiments, in which sets of local and distal cues are rotated relative to each other around a circular track, have shown that activity in the CA3 subregion is significantly more coherent than in CA1 [3]. Thus, it is critical to our understanding of hippocampal function to have models of spatial coding that can explain graded remapping as well as all-or-none complete remapping. While somato-dendritic dual-oscillator models have been examined [4, 5], it is not clear how to couple them with environmental cues to explore these sorts of effects. We demonstrate a more recent generalization of oscillatory interference models featuring multiple oscillator inputs [1]. Each oscillator's phase is modulated by the velocity vector of the trajectory such that the population phase code provides stable path integration.

First, we show that arbitrarily connected output units can produce spatially-modulated activity. Second, we demonstrate a cue-based phase-code feedback that represents learned fixed-points of the trajectory. This makes spatial representations robust to noise, but also allows cue manipulations similar to double-rotation experiments.

Double Rotation

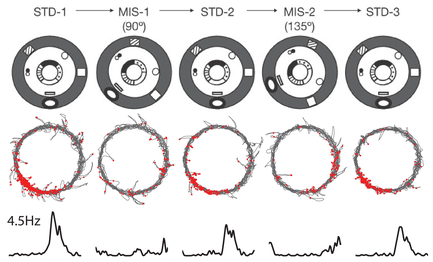

Fig. 1. Schematic of the double-rotation experimental paradigm in which sets of local and distal cues are put into conflict. Mismatch (MIS) sessions presenting cue conflict are interleaved with standard (STD) sessions presenting the familiar cue configuration. The spiking activity (middle) and linearized firing rate maps (bottom) of a CA3 place cell (rat 72, day 1, tetrode 11, cluster 8 from [3]) are shown across the five sessions of an experiment.

Coherent Local Control in CA3

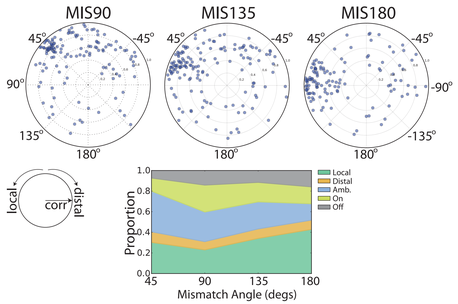

Fig. 2. Single-unit responses of CA3 place cells (N=5 rats, data recorded by I. Lee [3] and J. Neunuebel) across varying angles of cue mismatch. The rotation angle corresponding to peak firing-rate correlation for each place cell is plotted against that peak correlation (top row) to show that most CA3 place cells follow the counter-clockwise rotation of the local cues while maintaining coherent place fields. The proportion of locally controlled units is substantially larger than distal across tested angles (bottom).

Population Correlation Shift

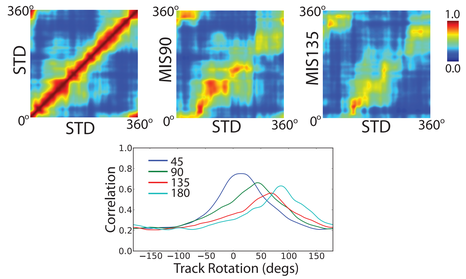

Fig. 2. Population auto-correlation matrix for the STD session (top left) and cross-correlation matrices with the 90- and 135-degree MIS sessions (top middle, right). Data aggregated across N=5 rats (I. Lee [3] and J. Neunuebel). The coherent rotation of the population code is evident in the shifting diagonal band of correlation in the cross-correlations. These diagonal correlations are linearized (bottom) for visualization of the peak correlation shift.

Oscillatory Interference

Governing phase equation for array of *N* velocity-modulated theta oscillators:

$$\frac{\mathrm{d}\vec{\theta}}{\mathrm{d}t} = \omega_0 + \vec{v}_t \cdot \mathbf{M}$$

where, for preferred directions ϕ and spatial scales λ,

$$\mathbf{M} = \begin{bmatrix} \cos(\phi_0)/\lambda_0 & \cos(\phi_1)/\lambda_1 & \cdots & \cos(\phi_N)/\lambda_N \\ \sin(\phi_0)/\lambda_0 & \sin(\phi_1)/\lambda_1 & \cdots & \sin(\phi_N)/\lambda_N \end{bmatrix}$$

and phase modulation is driven by the velocity vector of the animal's trajectory through the environment:

$$\vec{v}_t = \langle v_x(t), v_y(t) \rangle$$

This form of path integration provides a stable spatial signal, in the absence of noise, in the amplitude envelope of summation of multiple oscillators.

From a real circle-track trajectory, we use the velocity vector over time,

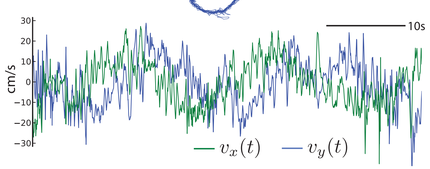

to modulate the phase of the oscillators such that varying synchronicity among the oscillators produces stable spatial fluctuations:

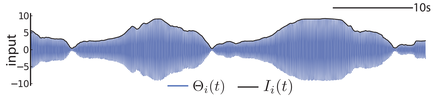

where the summed input oscillations for some output unit *i* is

$$\Theta_i(t) = \Sigma_{j=1}^{N} w_{ji} \cos(\theta_j(t))$$

with the signal envelope

$$I_i(t) = |\mathcal{H}(\Theta_i(t))|.$$

Model Place Cell Activity

Mapped back to the trajectory, the peak synchronization of the input oscillators provides the local spatial activity necessary for a place field.

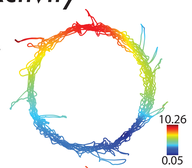

A threshold then determines output firing rate:

$$R_i(t) = \lceil I_i(t) - \mathrm{thresh} \rceil_+$$

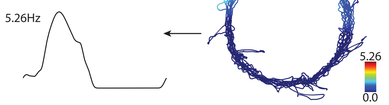

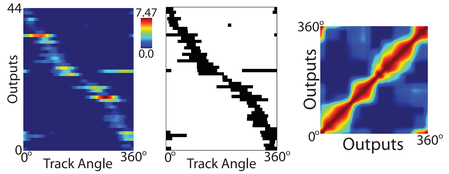

Fig. 3. Population responses of active place units from a simulation of 100 randomly connected outputs and 1000 theta oscillator inputs with 5% feedforward connectivity (bottom row). Firing rate response matrix (left) and place-field delineations (middle) are shown, in addition to the spatial auto-correlation matrix (right). The output of the multiple oscillator model qualitatively matches the sparsity and place-like activity of rat hippocampus.

Cue-Driven Phase Feedback

We add negative feedback terms to the phase equation for both local and distal sets of external cues:

$$\langle \Delta\vec{\theta}_{\mathrm{X}} - \Delta\vec{\theta}_t \rangle_{<\pi},\ \mathrm{X} \in \{\mathrm{loc}, \mathrm{dist}\}$$

so the phase equation becomes

$$\begin{aligned} \frac{\mathrm{d}\vec{\theta}}{\mathrm{d}t} = \ & \omega_0 + (1 - C_{\mathrm{loc}} - C_{\mathrm{dist}})\vec{v}_t \cdot \mathbf{M} \\ & + C_{\mathrm{loc}} \langle \Delta\vec{\theta}_{\mathrm{loc}} - \Delta\vec{\theta}_t \rangle_{<\pi} + C_{\mathrm{dist}} \langle \Delta\vec{\theta}_{\mathrm{dist}} - \Delta\vec{\theta}_t \rangle_{<\pi} \end{aligned}$$

where C is a cue-interaction coefficient modulating the phase feedback, $\Delta\vec{\theta}_{\mathrm{X}}$ is a learned phase target for the currently active cue (targets are stored on a training lap), and $\Delta\vec{\theta}_t$ is the phase code at time *t*.

Cue Representation

Fig. 4. Trajectory plots of the currently active cue (left) and the coefficient of cue-interaction (right) for an example cue configuration consisting of four small cues. Cues are evenly distributed around the track and local and distal cues are offset so that they are interleaved within STD (non-mismatch) session simulations.

Cue Conflict Response

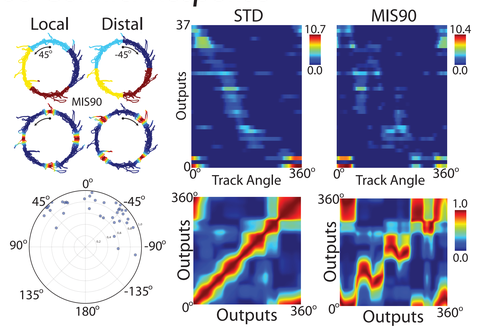

Fig. 5. Population response changes to an example double-rotation mismatch simulation where local and distal cues (top left) are rotated 90° relative to each other. Responses (right) are shown as population ratemaps (top) and auto- and cross-correlation matrices (bottom). Single unit rotations and peak correlation (bottom left) demonstrate both local and distal cue control with this symmetric cue configuration consisting of relatively small cues.

Asymmetric Cue Configurations

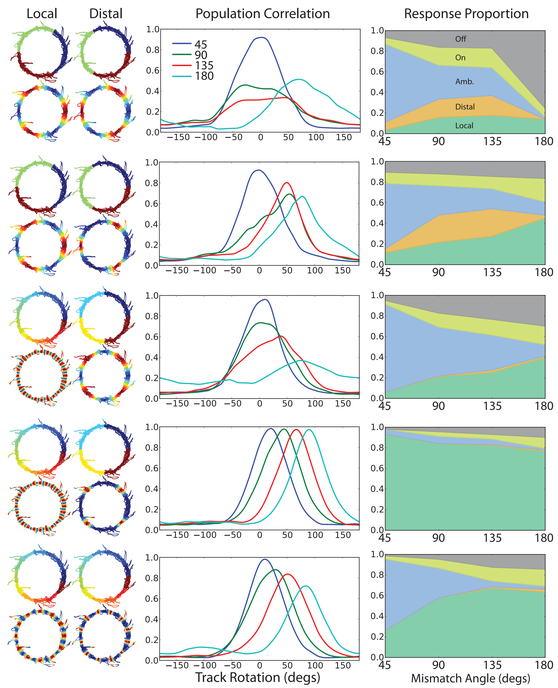

Fig. 8. Population correlation shifts (middle) and unit response change proportions (right) are shown for a variety of cue configurations (left). Different cue representations enable differences in population code coherence, cue-following and remapping characteristics across mismatch angles. Cue asymmetries are shown here in cue size (compare first and second rows) and in the number of cues (last three rows). Large numbers of small cues enable frequent updating of the phase code relative to local cues and is able to provide consistent local cue-control as seen in CA3.

Response Dynamics

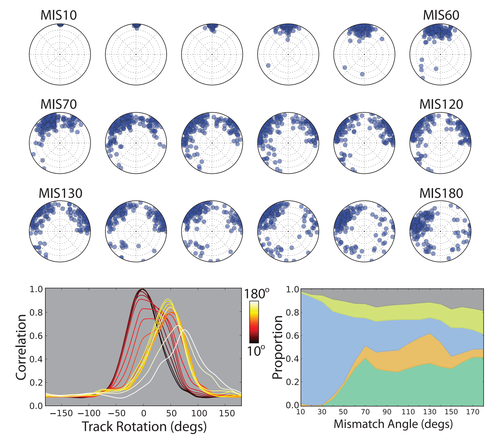

Fig. 9. Using the same cue configuration as the second row of Fig. 8 (three local and distal cues, with larger local cues), the mismatch simulations were performed at increments of 10-degrees. Single-unit rotations and peak correlations (top rows) show the emergence of both local and distal cue followers, though more follow the larger local cues. The population correlation shifts (bottom left) and response distributions (bottom right) show stable points in the response changes.

Conclusion

Simulating double-rotation using actual trajectories, we found that the diversity of remapping behavior among the output population depended on the number of cues, the feedback gain and the relative contributions of path integration and phase-code feedback. We found a diversity of both cue-following and ambiguous outputs qualitatively similar to the experimental data using moderate overall feedback gain and a small number of moderately sized cues. Further, asymmetry in cue configuration can bias mismatch responses similar to the local cue control exerted on CA3 place cell activity.

Recent intracellular recordings of place cells demonstrated increased theta power within-field and intracellular phase precession relative to extracellular theta [2], both of which result from this model. The multiple oscillator model provides insight into phase code mechanisms that may underlie a wide array of rate and temporal coding effects and remapping phenomena in hippocampus.

Acknowledgements

We thank Josh Neunuebel and Inah Lee for providing the CA3 recording data. This work was supported by PHS grants R01 NS039456 and P01 NS038310.

References

[1] H. T. Blair and K. Zhang. Place cells from theta rhythm: A many-oscillator model of path integration by phase interference. Society for Neuroscience Abstract, 192.27, 2009.

[2] C. D. Harvey, F. Collman, D. A. Dombeck, and D. W. Tank. Intracellular dynamics of hippocampal place cells during virtual navigation. Nature, 461(7266):941–6, 2009.

[3] I. Lee, D. Yoganarasimha, G. Rao, and J. J. Knierim. Comparison of population coherence of place cells in hippocampal subfields CA1 and CA3. Nature, 430(6998):456–459, 2004.

[4] J. O'Keefe and N. Burgess. Dual phase and rate coding in hippocampal place cells: The- oretical significance and relationship to entorhinal grid cells. Hippocampus, 15:853–866, 2005.

[5] M. E. Hasselmo, L. M. Giocomo, and E. A. Zilli. Grid cell firing may arise from interference of theta frequency membrane potential oscillations in single neurons. Hippocampus, 17(12), 1252–1271, 2007.

[6] J. O'Keefe and J. Dostrovsky. The hippocampus as a spatial map: Preliminary evidence from unit activity in the freely-moving rat. Brain Research, 34(1):171–175, 1971.

[7] J. O'Keefe and M. L. Recce. Phase relationship between hippocampal place units and the EEG theta rhythm. Hippocampus, 3(3):317–30, 1993.